Analysis and Modeling of the Hydro-Mechanical Behavior of Ain El Hammam Landslide, Algeria

Fazia Boudjemia* and Bachir Melbouci

Laboratory of Geomaterials, Environment and Installation (LGEA), University of Mouloud Mammeri - Tizi-Ouzou, Algeria

Abstract

A detailed analysis of the slope of Ain El Hammam, located at 50 km south of Tizi-Ouzou, revealed a complex landslide mechanism. The complexity of this hydrogravity process lies in its heterogeneous operating mode over time and its location in an urbanized environment. The study of the triggering factors and parameters that control the evolution of this instability is a very important stake in understanding the process of this landslide. The analysis made it possible to evaluate the relative influence of the geological, hydrogeological and geomorphological parameters behind the triggering of this landslide.

The current work included a numerical analysis of the behavior of the slope under various geotechnical and hydro-mechanical conditions. A numerical modeling of the slope was thus carried out using the FLAC 2D and OptumG2 softwares. The stability calculation provides safety factors indicating the existence of a superficial slip, a deep slip, and a very deep potential rupture. This allows for the association of the failure mechanisms with the observations made in situ. In addition, the results highlighted the important role of fluid overpressures in the triggering and amplification of the landslide, as well as the aggravation of the phenomenon by the overload due to the urbanization of the site.

1. Introduction

Among the land movements suffered by several regions of the wilaya of Tizi-Ouzou (Guirous et al., 2014; Bouaziz and Melbouci, 2019), the landslide of Ain El Hammam has attracted a maximum attention since its appearance, given its complexity and the important disorders that have generated it. Marked by exceptional climatic events, the landslide is a steep slope composed of metamorphic soil, and is characterized by slow yet extended movements with episodes of acceleration.

Several studies and investigations have been carried out in order to better understand this phenomenon, and seek a comfortable solution. This work (LNTPB, 1973; GEOMICA, 2006; 2009 and ANTEA, 2010) includes essential knowledge which deals with the recognition of this site. A number of assumptions emerged in relation to the origin of the landslides, the mechanisms of failure, and the composition of the grounds which moved. All these ideas make it possible to set up a full description of this phenomenon, and to define the physical and geometrical parameters and the mechanical factors to be taken into account during a modeling.

Numerical calculations of the slope stability (Talren 4) carried out by the ANTEA laboratory (2010), assume the existence of surfaces of discontinuity at several depths of the slope, with a rotational fracture geometry.

Moreover, the modeling of landslides is based on a multidisciplinary approach that derives from distinct conceptions. These include on one hand, the visual analysis of the natural sites, which includes the classification of the types of slip and designation of volumes of the soil masses, affected by the movements, and on the other hand, the deterministic analysis which defines the properties of these moving massifs and their introduction into mathematical models.

In the first part of this work, an overall description of the phenomenon and its probable origins has been presented. In the second part, a numerical modeling has been used to reproduce the hydro-mechanical conditions, inducing the instability of the slope, and analyze the relevance of the different fracture scenarios.

2. Description of Landslide

The detection and auscultation of land instabilities and the potentially unstable zones in Ain El Hammam region require a methodology based on a few tools including existing documents, mapping techniques, and direct observation of the study sites (Pisani et al., 2010; Wu et al., 2019).

With a heavy past in terms of ground movements (since 1969), the slope presents a chaotic and a bloated aspect reflecting the fragility of the site and its sensitivity to the evolution of the forms of the relief, by conjugate sets of erosion and deformation due to both subsidence and landslides as well as to earthy flows. Indeed, one can observe several scars of former superficial or semi profound slides which would have led to displacements of voluminous rocky panels. This activity marked the morphological modification and the fragile equilibrium of the entire slope which went through a long period of relaxation.

This situation has led to the concept of several reactivations caused across time (1973, 1984 and 1986), by climate change and inappropriate human intervention. The first estimates of the magnitude of the movement describe an

---

* Corresponding author e-mail: b_fazia78@yahoo.fr

extent of a 90 m width with a vertical drop reaching 20 m, for an unstable layer with a small thickness which concerns only embankments and materials resulting from the alteration of schist (LNTPB, 1973). These first signs of instability that appeared in the high side of the slope during the process of urbanization have been studied in order to develop a POS (ground occupation plan) which will prohibit high-rise constructions on the affected part by slippage.

Towards the nineties 1990 , after the removal of long and thick thrusts, instabilities were reported, at the bottom of a primary school. This school experienced major disorders then even on its structural frames.

The stability of the site became then fragile until 2002 and 2004 when new disorders reappeared and the movement kept evolving until 2006.

Stretching over 150 m in length between the summit and the frontal part of the slope, the slip began to describe a more complex form until it reached some of the slope on the south-east side beside the road leading to Ait Sidi Said (Figure 1).

The major part of the landslide affects the urbanized area, and many infrastructures are consequently affected. It also affects roads that lead to various localities. Boulevard colonel Amirouche, which constitutes the main axis of regional communication, shoemaker's street, and Bounouard Street, are constantly threatened and degraded.

Figure 1. Propagation and evolution of the slide downstream of the slope.

During winters with heavy rains, the movement of the land continued to spread in a strong and steady manner. In the winters of 2008-2009, some particular and marked disorders appeared, such as a distortion of buildings and retaining walls (Figure 2), and also crevasses on the roadways (Figure 3).

During winter of 2009-2010 the activity of the sol was closely monitored, following the propagation of the movement towards the median and lower zones of the slope (Figure 4). Prospecting work has been initiated since October 2009 by setting up a network of points subject to topometric measurements in order to define the kinematics of the movement (displacement reaching 50 cm over a few zones during a period of six months).

Figure 2. Obstructions observed in buildings.

Figure 3. Dislocation of a retaining wall, subsidence of sidewalks, and cracks in pavements affecting pipeline networks.

Given the great influence of water on these movements, it has been decided since 2012, to set down a diversion system for runoff water and waste water towards the downstream slope of the area. The slippage, then, slowed down to leave behind very slow movements which characterized a calm period. This, without neglecting the new local instabilities, appeared in particular, on the Shoemaker street (Figure 5), as well as during the renewal of numerous cracks in the retaining walls and ways, which are filled in by public services each time.
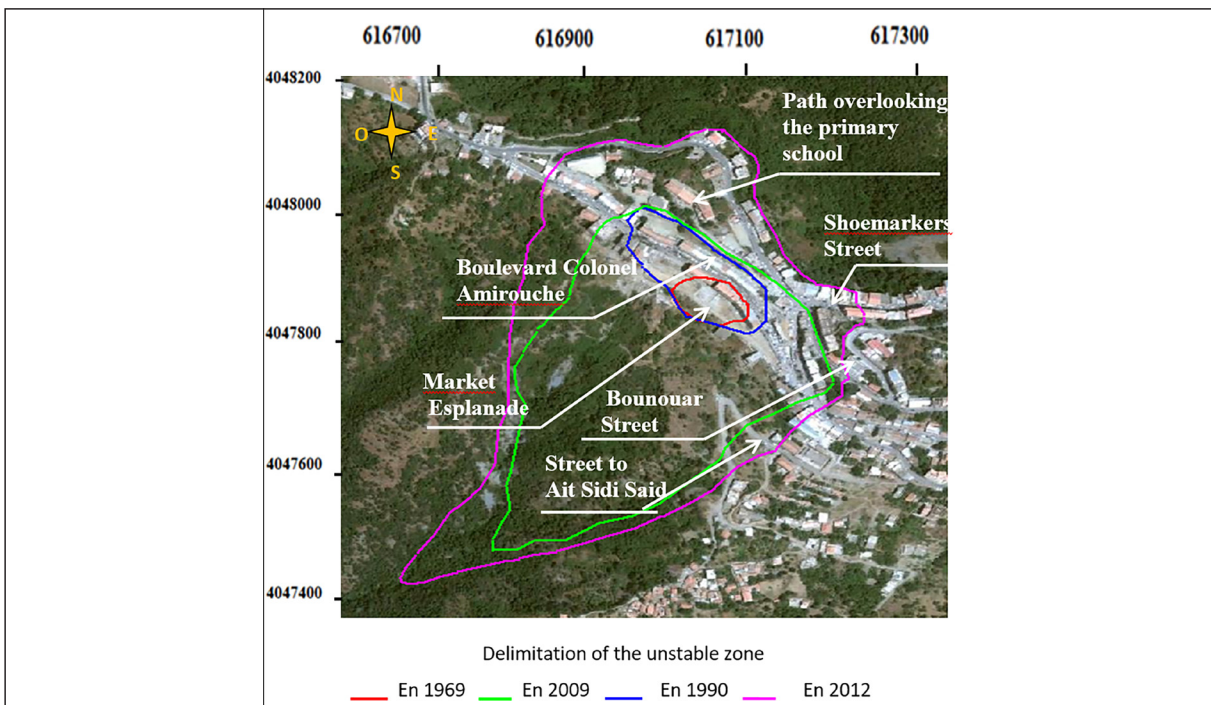
Figure 4. Evolution of the area of landslide (Djerbal and Melbouci, 2013), and locating the principal places affected by the movement.

Figure 5. New instabilities registered in 2016.

The current monitoring marks a reactivation of the movement under the influence of bad weather recorded in January, 2019. This was observed, in particular, on two buildings in R + 4 which lean towards the market, below, increasingly each day, especially following showers. The adjoining building shows a gap of more than one meter, at the fourth floor, which continues to cause concern to the local population who fear that the impact of this movement may cause the collapse of these buildings at any time.

3. Origins of Landslide

The origins of the landslide of Ain El Hammam are probably multiple and remain polemic. Indeed, it is a convergence and conjugation of several factors that can be categorized into three groups of factors: predisposing factors, triggering factors, and aggravating factors (Tullen, 2002; Ietto et al., 2018).

3.1 Predisposition Factors

These factors act through multiple intrinsic conditions of the slope. The topography of the site is characterized by a steep slope, with varying inclines over the entire slope, giving rise to high instability potentials.

The geological nature of the schist formations defines the altered layers at depth, giving rise to underground water circulation which contributes to the reduction of the mechanical strength of materials. These formations are overcome by deposits resulting from the continuous erosion of the slope and a succession of embankments. These deposits form a superficial cover which, by its permeability, contributes greatly to the setting up of preferential channels linked to the infiltration of water, thus promoting the phenomenon of the regressive alteration of the schist.

The geotechnical characteristics define the high clay mineral contents (Kechidi, 2010) and materials that are less resistant, but sensitive to the phenomena of ground movements.

The hydrogeology of the site, is sustained by the presence of several water sources and streams of torrential and permanent flows, which through their erosive action, lead to a decrease in mechanical parameters and a modification of the morphology.

The effect of deforestation also plays a significant role. Landscape areas are characterized not only by a poor vegetation cover, but are also shaved over the urbanized area. In general, vegetation contributes to the stabilization of the slopes by fixing the soil and modifying the water balance (Dapples, 2002; Ismail et al., 2018).

3.2 Aggravating Factors

Land use is the main aggravating factor in Ain El Hammam's landslide, it is basically linked to the development and increasing urbanization of the region. This action of anthropic origin, participates strongly in the degradation of the stability conditions. In this context, the appearance of new disorders around 1990 during the construction of the BDL building can be mentioned. This was noticed as a lowdown period of the landslide process, notably on the upstream side since the demolition of some buildings in 2009. Anthropogenic action is also manifested by the modification of the morphology of the slope induced by the significant earthworks leading to the suppression of natural abutments as well as by the inappropriate jets of embankments contributing to the design steeper slopes.

3.3 Triggering Factors

This part is linked to the climate side which is favorable to landslides. The mean annual rainfall value for this area is 1058 mm between 1968 and 1994, and 1009 mm between 1997 and 2006. This value corresponds to the values of a very rainy region. However, it was found that the most significant trigger and acceleration of the movement are largely conditioned by extreme weather events; for example, the first signs of movements were observed in December, 1969 after a heavy rainfall. The new disorders during 2004-2005, their spread along the crown and on the slope, and also the paroxysm of the displacements in winter of 2008-2009 have also appeared following a heavy rainfall.

As far as snow, that characterizes the region, is concerned, it appears to be important, in particular, in the winters of 2005 and 2012. Its spread over long periods causes the disintegration of the underlying layers by frost, but when melting, it causes saturation of the soft layers and then setting in motion in the short term.

4. Geological Overview

The district of Ain El Hammam belongs to the internal zones of the chain of Maghrebides. In this area, the Kabyle crystallophyllian base was found to be mainly composed of metamorphic massifs, namely, gneisses, marbles, micachists, and schists (Figure 6). This base is, in some places, unconformably covered by detrital deposits of the upper Oligocene-lower Miocene age, named Oglio-Miocene kabyle (Durand-Delga, 1969).

In the region of Ain El Hammam, the crystallophyllian basement consists of micaceous schists which were seen on 78.91% of the territory of the commune. The rest is occupied by granite schist (10.66%), gneissic granulites (6.98%), fossiliferous schist, and phyllades (3.16%), to which can be added the quaternary formations corresponding to the filling by alluvium deposits representing 0.29% of the total area.

The geological formations, therefore, include a series of essentially schistose rocks with micaschists dominated by a satin schist feature of a dark gray color. The latter are sometimes in contact with gneisses, and have a mean directional schistosity ENE-WSW. The axial dipping of this formation is oriented towards the south-east with a maximum dip of 60 °. The micaschists are dark cream to light brown; their schistosity takes the same direction as that of the schists, which varies from 30 ° to 80 ° towards the south.

On the slip zone, a detrital sequence of grayish satin schists, containing fine quartzite-rich levels and a predominantly clayey-silty cover, constituting the upper unit (Figure 7).

The nature of the surface structure and the basic formations which are perceptible to the fracturing in the upper part constitutes a geological context very favorable to the movements of ground.
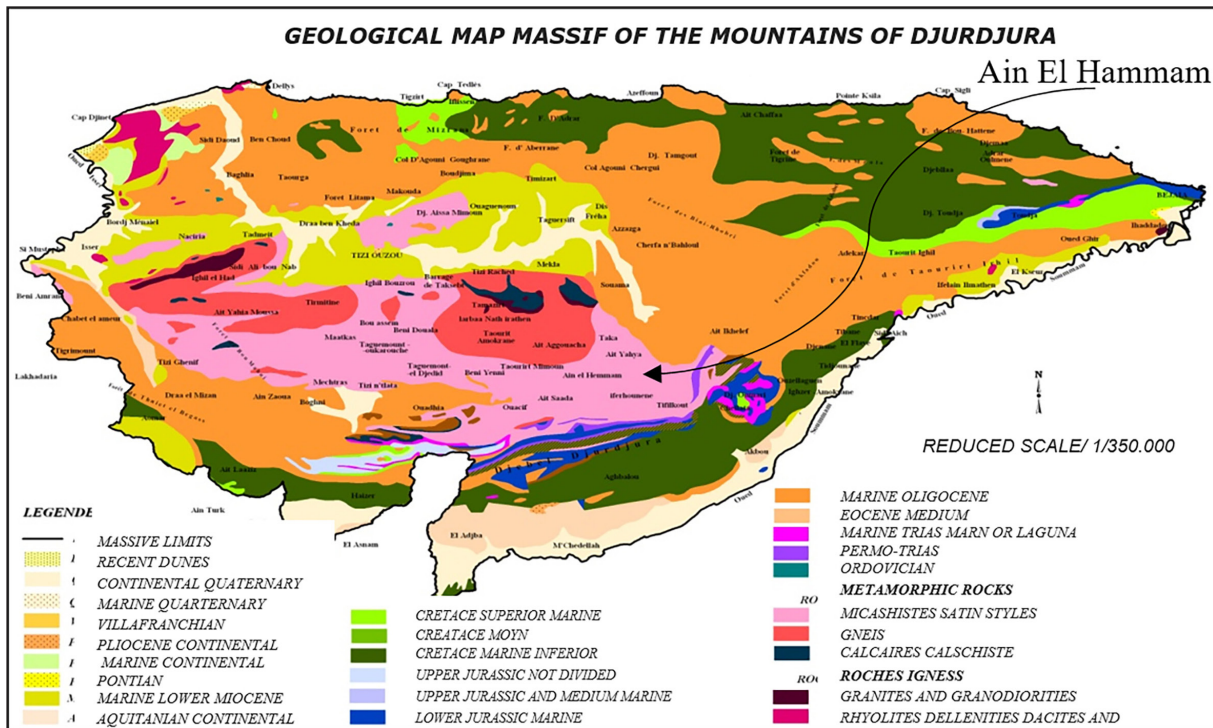
Figure 6. Geological map showing solid masses of the mounts of Djurdjura (CENEAP-MATET, 2010).
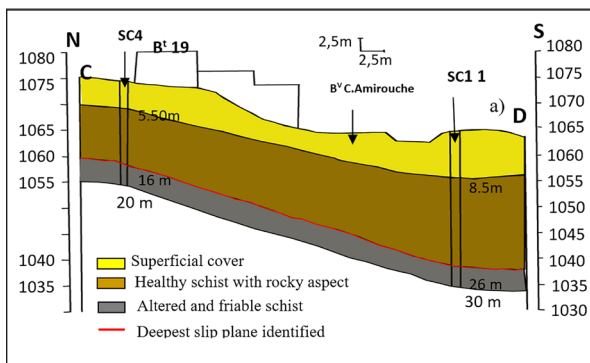
Figure 7. Geological section made by GEOMICA laboratory (2009)

5. Modeling of the Landslide

Numerical simulations were conducted by two soft wares; Optum G2 enables the use of the two methods of limit analysis: the outer side approach (Upper) (Michalowski, 1995) and the internal side approach (Lower), and Flac (2D) 6.0 using the finite difference method, and is based on the continuous medium approach. The choice of this approach is explained by the presence of layers of loose materials and highly fractured materials, surmounting a rock mass that does not contain significant fractures justifying the use of discontinuous models. It is noted in this context, that the rock behaves as a continuous medium in the case of a massive rock without any family discontinuities; or as a continuous equivalent, in the case of fractured rock with several families of discontinuities (Bemani Yazdi, 2009; Billaux and Dedecker, 2018).

5.1 Justification of the Two-dimensional Model

In the absence of complex or particular topographic shapes (convex or concave forms) along the slope subject to numerical modeling, the two-dimensional simulations can be representative of his real behavior. The visual observations of the site's morphology, the direction of movement, and the examination of topographic surveys suggest that the three-dimensional effects of the model will not be very significant, a two-dimensional profile (Figure 8) was, therefore, chosen.
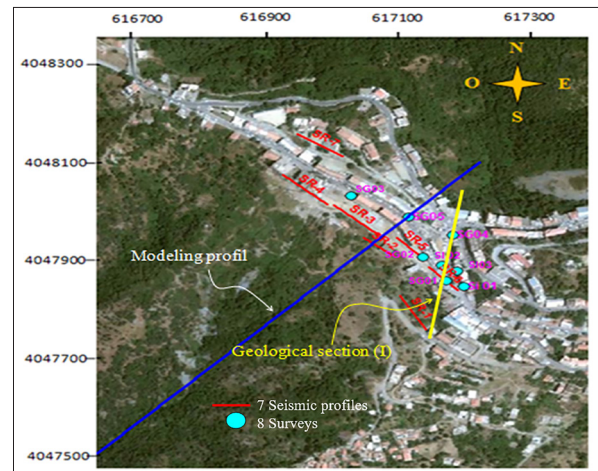
Figure 8. Locating the profile used in the modeling and the geological section defined by figure 7.

5.2 Calculation Assumptions

- The superficial formations are considered to be homogeneous over the width of the profile.
- All materials behave on the scale of the slope as a continuous medium.
- The flow of interstitial waters is assumed to be parallel to the slope.

5.3. Lithology and Geotechnical Characteristics

The section of the slope is represented from top to bottom by the tratigraphic formations below (Figure 9) using the geotechnical characteristics defined by the Mohr Coulomb rupture criterion (Table1).

- A clay-silty cover with a thickness of 3.5 to 10 m.
- A layer of altered schist with a thickness of 20 m.
- The compact satiny schist that constitutes the rock substratum.

These geotechnical and lithological characteristics were determined through various soundings carried out by the GEOMICA laboratory (2009).
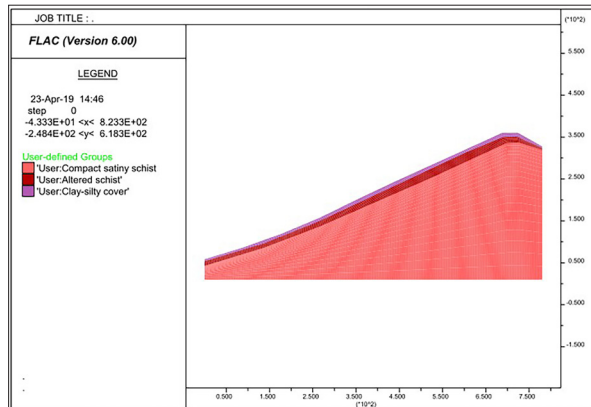
Figure 9. Calculation model.

Table 1. Principal physical and mechanical parameters of materials.

Geotechnical parameters	Surface layer	Intermediate layer	Rock substrate
Unit weight γ [kN/ m3]	19.60	19,90	22,00
Modulus of volume deformation K [kN/m²]	410735	539824	2451000
Shear modulus G [kN/ m²]	157500	207000	939850
Cohesion C [kN/m²]	18	40	2000
Friction angle φ [°]	36	34,06	14,3
Angle of dilatation Ψ [°]	0	0	0

6. Stability Analysis and Amplitude of Displacements.

Similar to all methods of preventing landslides, stability analysis remains an essential tool for assessing the danger of these phenomena. However, the estimation of the safety with respect to the risk of rupture is encountered by a major difficulty (Dadouche et al., 2008; Gravanis et al., 2014), since it requires careful recognition of the geometric and mechanical quantities as well as the geological structure. However, it should be noted that the effectiveness of the results is also assessed by choosing the method which defines the safety factor, through which one seeks to quantify the stability state of a natural slope by a single number. This results in several definitions, the choice of which is generally included in the selection of the calculation method (Faure, 2000).

6.1. Recommended Methodology

Numerical simulations were conducted by sensitivity tests to variations of the mechanical properties of materials, loading ways and hydraulic boundary conditions. The purpose is to know the role of each of these parameters in the triggering of instabilities and on the amplitude of the displacements undergone by the ground set in movement, as well as to define the modes of rupture.

This work, therefore, proposes to vary these different parameters over a wide range of configurations combining the different situations, while seeking a level corresponding to the limit equilibrium (critical level that marks the start of instability).

The study must, therefore, firstly provide decisive results of the main factors leading to the triggering of the instability of the slope and those leading to the aggravation of the sliding process. Secondly, the various mechanisms of rupture that are likely to take place at the level of the slope must be determined.

Several configurations of the parameters have been developed. Flac defines a single value of the safety factor, which corresponds to a breaking or potential breaking surface defined by the fields of shear deformation rate. Optum develops a rupture defined by the fields of energy dissipation by shear. The three calculation methods are all based on the reduction of the mechanical parameters. The safety factor is in this case defined by

$$Fs = \frac{C}{C_{critique}} \text{ or } \frac{tang\varphi}{tang\varphi_{critique}}.$$

Furthermore, during the calculations using the Flac software, the maximum amplitude of vertical and horizontal displacement was recorded for some of the proposed configurations.

6.2. Comparative Study of Calculation Methods

Before analyzing the stability results, it is necessary first to examine the results of the comparison of the safety factor values (Figures 10 and 11) obtained by the three calculation methods.

As preliminary remarks on this subject, the three curves retain the same pace over all the ranges of the chosen parameters and sometimes nearly touch them. Although the Flac software underestimates the stability of the slope compared to the limit analysis methods, the three methods give very close safety factors, and estimate, in the same way, the stability of the slope. For example, using the three methods, the limit equilibrium (Fs = 1) is reached practically with the same parameters.
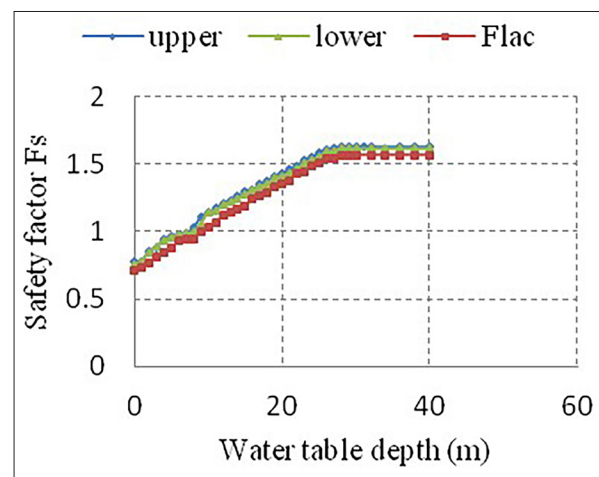
Figure 10. Comparison of the curves of variation of the safety factor as a function of the water table depth obtained with the three calculation methods.

Moreover, it is evident that the static method gives values of the safety factor lower than those obtained by the kinematical method. In fact, the first seeks a lower bound value of the safety factor using a field of stresses, whereas the second determines an upper bound value using a field of displacements or velocities. In result, the search for the lower and upper boundaries makes it possible for each

configuration to bound the safety factor that defines the real state of stability (Cubas, 2009; Li et al., 2016).
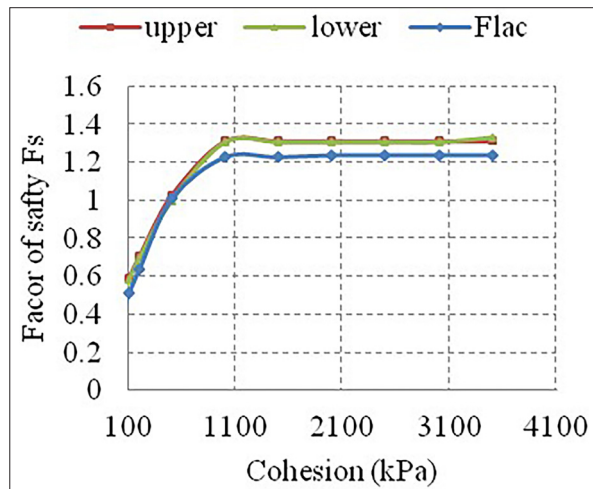
Figure 11. Comparison of the curves of variation of the safety factor as a function of cohesion with the three calculation methods.

6.3. The Role of Water

Calculations of the safety factor Fs and the corresponding displacements are carried out through a wide range of configurations which represent more or less effective precipitation; the results have clearly illustrated the significant role of the hydraulic parameter. In fact, it is quickly noted that with the fall down of the water table, the safety factor Fs increases progressively along the first part of the curve (Figure 12), on which a linear increasing of Fs is mostly seen with the increase of the depth of the water table until 28m.
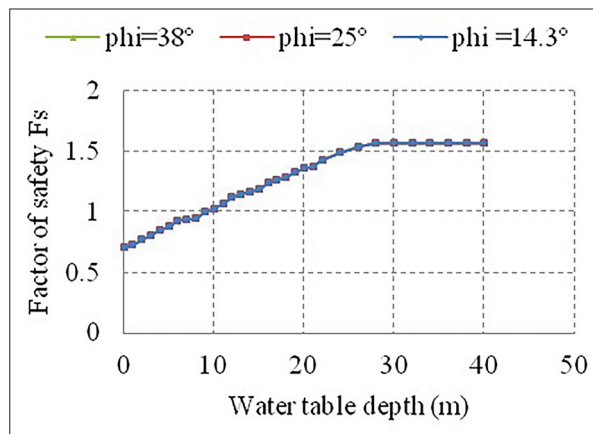
Figure 12. Curves of variation of the safety factor as a function of the water table depth.

Over 28 m, Fs remains constant (horizontal curve) and equals 1.57 (Fs = 1.57), This value corresponds to the same state of stability as that found in the absence of the water table, which means that after this depth, water has no effect on the stability of the slope. It must be noted that this level corresponds to the interface delimiting the bedrock and that this is considered as a continuous medium.

For variations, of maximum horizontal and vertical displacement values with the increment of the depth, the curve (Figure 13) marks a quick and intense fall down of displacement with the depth of water table between the ground surface until 4m depth. Underneath this level,

there is a second stage throughout displacements which is diminished slowly to be cancelled out at a 9 m depth where the slope has experienced the limit state of stability.
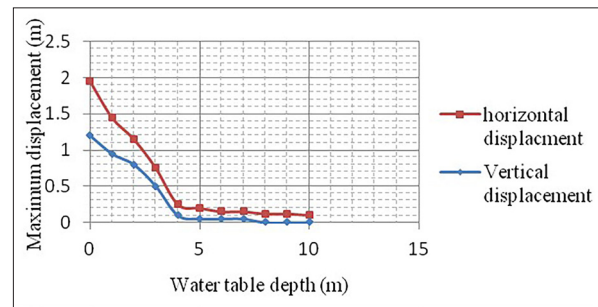
Figure 13. Curves of variation of horizontal displacements and vertical displacements as a function of the water table depth.

It should be pointed out that over the whole range of the water table depths, the horizontal displacements are greater than the vertical displacements; the maximum amplitude for the horizontal displacements has occurred at the frontal part of the ridge.

Several piezometric heights are, therefore, considered at the slope: important ($0 \leq h \leq 3$ m), moderate ($3 < h \leq 8$ m), medium to low ($8 < h < 16$ m), very low (h> 16 m). This choice can be explained by fluctuations in the water supply during seasonal variations.

The first level corresponds to a complete or partial saturation during periods of intense and long-lasting rainfall and also of massive and slow snowmelt. This represents the worst hydraulic conditions, resulting in superficial instability with very low safety factors, which vary from 0.75 to 0.8, and a large maximum displacement varying from 0.75 to 2 m in the horizontal direction and from 0.5 to 1.2 m in the vertical direction.

The moderate height represents a water table located between 4 and 7 m deep; however, at this level, the calculations always give a low safety factor, not exceeding 0.98, in spite of the strong cohesion of the materials. On this range, the slope remains unstable, but presents displacements less sensitive to the variation of the piezometric height.

With a water table situated at a 9 m depth, the FLAC software shows that a slope in a state of limit equilibrium (Fs = 1), whereas with the OptumG2 software, this state is already reached at 8 m, and instability, thus, begins beyond this depth. Between this level (the limit equilibrium) and a depth of 16 m, stability is always considered precarious (Fs <1.25), so the movements can, thus, appear at this level, with the effect of other mechanical parameters.

The low level defines a piezometric height over 16m beyond which the slope is perfectly stable with safety factors exceeding 1.25.

In general, these results show the important role of water in the stability of Ain El Hammam slope, within large and moderate piezometric heights, which tend to reduce the safety factor by 55% and 40%, and to amplify the displacements in a significant way, in comparison with the results obtained in a dry state.

These conditions can be considered very realistic and representative of the instabilities recorded during periods of heavy rainfall, which led to the rise of the water table that

can reach the ground surface of the soil. It is noted that these situations lead generally to modifications of the mechanical characteristics tending to reduce their internal resistance forces.

Moreover, these results limit the depth of groundwater from which the instability begins (8 to 9 m) and the piezometric level over which water has no effect on stability (28 m).

However, these spacing distances must be analyzed in the presence of other unfavorable conditions, in particular, the modification of the mechanical characteristics and loading at the peak.

6.4. The Role of Mechanical Characteristics

As mentioned above, the characteristics determined in the laboratory for the superficial and intermediate layers have been assigned. The pure schist has not been characterized in the preliminary investigations. For this purpose, the variability of schist parameters over sufficiently broad areas have been taken into account in this study for a better understanding of the role of the mechanical strength of the fall of rock masses in triggering the instabilities.

It must be pointed out that compact schist is often characterized by a friction angle $\varphi = 14.3°$ and a cohesion value varying between 2000 and 3600 kPa (Chalhoub, 2010). These values should be guaranteed by all means to check out any modification of geological structure within the substrate that can lead to the degradation of the geotechnical characteristics, at least on the upper part.

In the study of the influence of the variation of the piezometric level, three calculations were carried out for each level of the water table, and for three values of the friction angle of the schist: $\varphi = 14.3°$, $25°$ and $48°$, while keeping the other parameters as shown in table 1. These angle values are chosen with respect to the tilt angle of the slope with an average of $25°$.

In this context, it should be noted that any increase in the friction angle alone does not offer any margin of safety even at fairly high values, thus, the safety factor is the same for the three values of φ in each piezometric level. This is clearly seen in Figure 12 where the three curves are merged.

At this stage of the study, it can be concluded that the variation of the friction angle of the rock masses alone does not influence the stability of the slope.

As far as cohesion C is concerned, calculations of Fs have been carried out for a wide range of values (C = 100, 200, 500, 1000, 1500, 2000, 2500 and 3500 kPa) which can define several types of shale, altered, compact and healthy one). For these C values, the analysis is made for three piezometric levels: high, medium, and low (h = 0, h = 9 and h = 26 m) (Figure 14) noting that in this variation of cohesion, the other characteristics are those defined in table 1.

For the low cohesion (C = 100 and C = 200kPa) corresponding to highly fractured schist, the safety factor remains low even at a sufficiently stabilizing piezometric level. These conditions correspond to circles of sliding so deep to the point that they can't be considered very realistic.

Although a small increase of C value (C = 500 kPa) leads to an improvement of the stability, this improvement, however, is very limited and is mainly dependent on the

level of the water table. In fact, when the soil is completely saturated with water, the safety factor is less than 1 within the entire cohesion range. From C = 1000 kPa upwards, Fs = 0.75, and it remains constant.
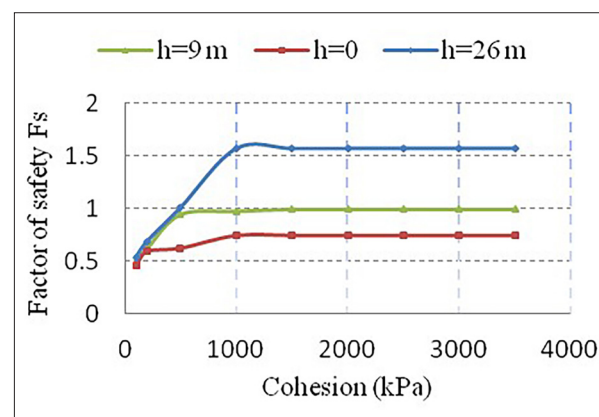
Figure 14. Curves of the coefficient of safety as a function of cohesion.

At a moderate piezometric height h = 9 m with a high C value (C≥1500 kPa), the state of stability is very critical. Consequently, the improvement of the cohesion alone does not give any satisfactory evolution of the state of stability.

This has led to study the variation of Fs with the variation of C for a lower piezometric height (water depth h = 26m).

In summary, the variation in cohesion at the rock level significantly affects stability regardless of the level of the aquifer considered, and the coefficient Fs increases constantly with the improvement of the cohesion. For example, a variation of the latter by 50% results in an approximate increase of 20% of the safety factor. However, the progression of cohesion from C = 1500 kPa upwards does not affect Fs which then depends only on the level of the water table.

6.5. The Influence of Upstream Loading

The action of overloading at the top of a natural slope by urbanization can harm its stability. Indeed, the additional weight of the constructions modifies the state of equilibrium of the slope, and can act as an aggravating factor, or a destabilizing factor.

However, the ridge of the slope of Ain El Hammam is a plate that continues to receive projects of more or less vital importance, which is undoubtedly a factor contributing to its instability.

This point has been taken into account in the calculations by considering a uniformly-distributed load on the peak of 100 kN/m² representing the approximate weight brought by buildings of the (R+5) type. This load application did not lead to any change in the safety factor (Table 2).

The amplitude of the displacements varies by 21% in the vertical direction at the slope points of height altitude = 1085 m to 1070 m, while no variation of this magnitude has been recorded in the horizontal direction. However, the effect of this load is remarkable not only by the excessive variation of the maximum displacement intensity, but also by the modification of the distribution of the displacement isovalue fields and of the areas going in plastic behavior by tension by shear and by volume deformations.

Table 2. Comparison of the results of the calculation of
the safety coefficient and the maximum displacements with or without upstream loading.

Loads (kPa)	Calculation software	Water table depth [m]	Without loads	With load of 100 kPa
Safety factor Fs	Flac	9	1	1
	OptumG2	9	1	1
Maximum vertical displacement [m]	Flac	0	-1.2	-1.7
Maximum horizontal displacement[m]	Flac	0	-2	-2

The results of this study investigate the spread off of the displacements and their progression downstream and upstream of the slope (Figure 15) as well as the appearance of a new sliding plane defined by the propagation of the areas that have over crossed the plasticity state (Figure 16). It should be noted that these zones had an elastic behavior before the application of the load.
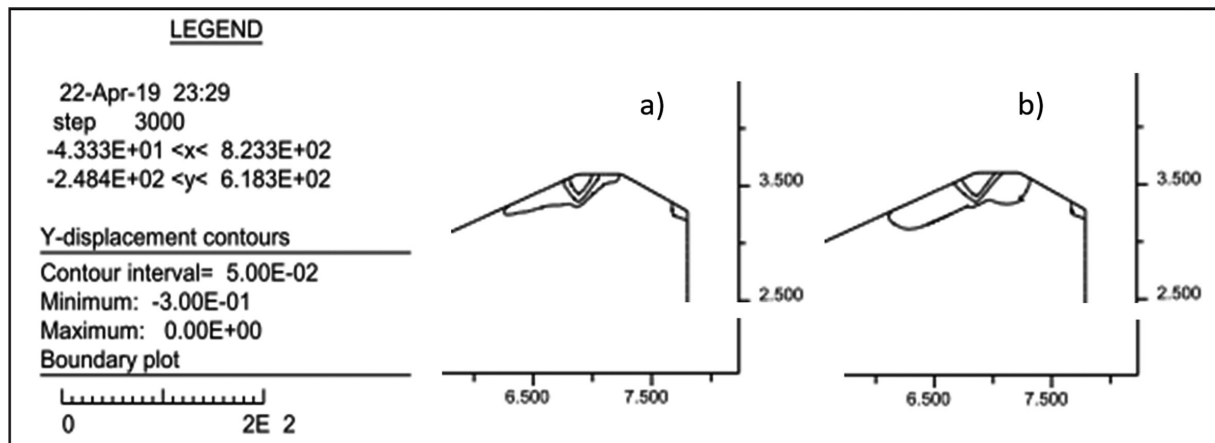
Figure 15. Isovalue lines of vertical displacements. (a) Before loading. (b) After loading.
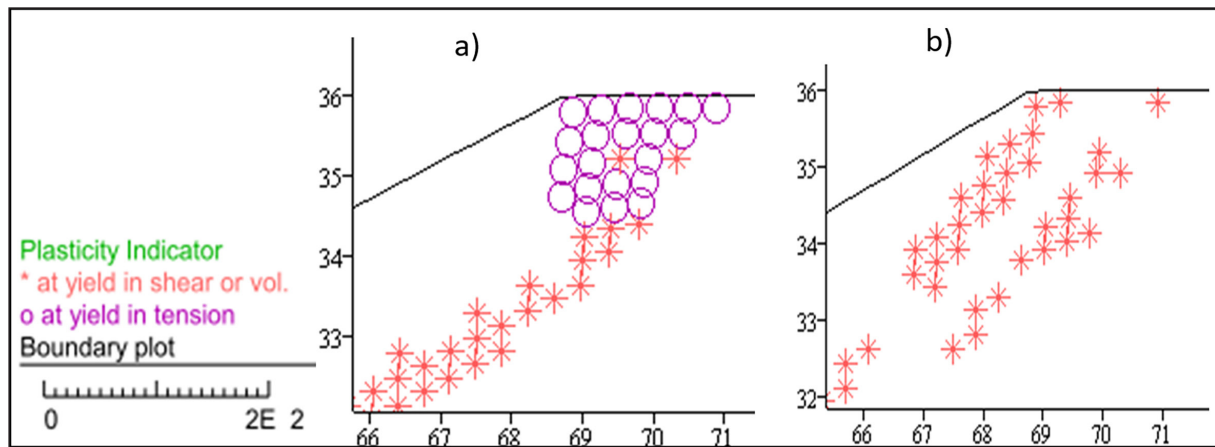
Figure 16. Areas of plasticity (a) Before loading. (b) After loading.

Finally, with the simulation of the loading due to urbanization, there is no change in the stability state of the slope. This can be explained by the weight of the overload being low compared with the massif one; therefore, this does not substantially affect the motive force. There is, then, no subsequent change in the ratio: motive force to stabilizing force.

If the overload alone does not lead to the instability of the whole slope, it can, however, influence the behavior of the massifs, the evolution of displacements and the modification of behavior significantly at the level of certain parts.

7. Analysis of the Failure Mechanisms

The large diversity in the behavior of the massifs and consequently in the failure mechanisms, results from the mechanical composition and the modification of the hydraulic conditions under the superficial effect of the concentrated runoff of the surface waters and by the internal erosion caused by groundwater in addition to the great variety of the geological structure describing the lithological nature of the rock matrix, the fracturing density, and the intensity of the alteration (Fleurisson, 2001; Wu et al., 2016).

An examination of the main results of calculations indicates that the distribution of the deformations shows a zone of concentration which corresponds to an instability of the slope undergoing a generalized movement towards the south of the region, accompanied by a slight collapse of part of the peak of the hill where the upper sliding limit is located. The downstream limit is linked to the mode of rupture obtained by the calculations and the extent of the sliding as well as the volume and the depth of the lands affected by the movement.

Different failure mechanisms have been highlighted during the calculation of the stability. For several situations, considered according to the mechanical parameters and the hydrogeological conditions, four main rupture configurations were detected (Figures 17-22), and their differences depend mainly on the drainage conditions and the cohesion of the rock mass.

7.1. Failure Mechanism 1

The short-term calculations carried out using the OptumG2 software, considering the water table level with the free face of the slope, show an instantaneous slip marking a plane rupture line along the superficial overlay-altered schist interface (Figure 17), along a 150 m length at a depth not exceeding 10 m. This configuration represents, on one hand, the hypothesis of the superficial slip envisaged by the ANTEA laboratory (2010), and on the other hand, the hypothesis of rupture 1 defined by Djerbal and Melbouci (2012). This type of slip can occur during winter seasons with heavy rains causing mobilization of the soft and completely saturated cover.
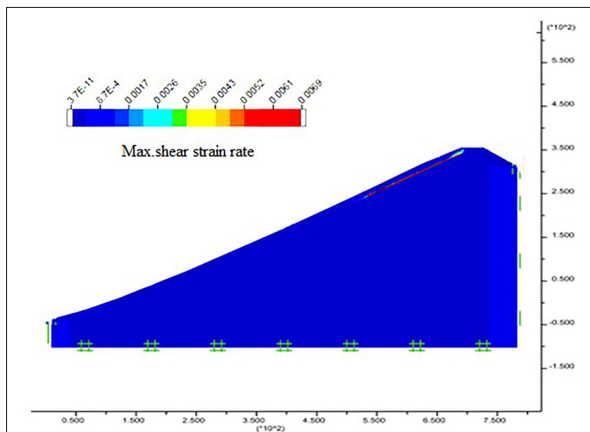
Figure 17. Failure mechanism 1 (Short term limit analysis).

7.2. Failure Mechanism 2

Regardless of the mechanical properties considered for the bedrock, using the Flac program combined with a significant piezometric height, many instabilities are registered along several sub-rotational rupture lines indicated by the concentration of the deformations and the direction of the displacement vectors (Figure 18). These results are consistent with the results of in-situ observations which show an encroachment of several landslides.

This configuration in an overall mean reflects a large-scale phenomenon that affects the entire slope along a 450 m length at a depth that can reach the limit of a non-altered schist.

For the mass set in motion, this study highlights the importance of the shear strain rate set on the upper part of the slope; a shear strain which decreases towards the foot of the slip, marked by the strain fields, with a reset downstream of each crack.

The direction of the displacement vectors, however, shows that there is a tension at the level of the urbanized part of the slope at the altitude of 1075m, which is well confirmed by the fairly deep-tension cracks observed on road RN 15 at the market place, and also below the constructions at the top of the slope (Figure 19).
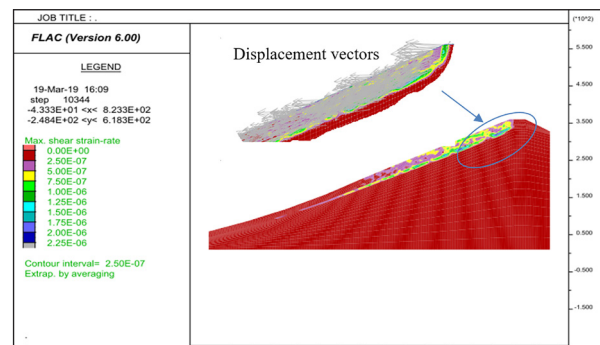
Figure 18. Tensile crack observed near a single structure at the top of the slope.

Figure 19. Failure mechanism 2 (finite difference analysis with a high piezometric height).

In general, the displacement vectors with regards to their direction show at least three lines of rupture initiated at the summit part of the slope. The first one spreads over a length of about 150 m, the second over 250 m, encroaching another plane sliding on the remaining part of the slope, with deformations decreasing without a net slip mark, but are delimited by the upward vector displacements at the 855m coastline.

7.3. Failure Mechanism 3

For the volume delimited by failure mechanism 2 (Figure 20), the drainage conditions surely modify the nature of the failure surface. In fact, with the drawdown of the water table to a 4m depth (h = 4m), and combined with relatively high cohesions (C = 1000 to 3500 kPa), the failure is located at the altered schist-healthy schist interface, and sets the superficial layer in motion as well as the whole slice of the altered shale within a large drop level (about 200m) and a length of 450 m. The displacement vectors show an overall downward movement in the direction of the slope, marking the foot of the slide at the altitude line of 900 m. This movement may be sustained by the smooth and plastic nature of the formation in contact with the healthy masses (Djerbal and Melbouci 2012), causing a considerable drop in the resistance of the overlying layers. Inside the body of the slip, the strains decrease by nearly 50% in comparison with failure mechanism 2.

In addition, the results of long-term calculations carried out by the OptumG2 software (Figure 21.a) represent the failure mode obtained for all probable hydraulic boundary conditions in association with the high mechanical strength of the existing schist. They make it possible to demonstrate a quasi-plane failure affecting an extended length of the slope. This failure starts on the front part of the slope contrary

to the result of calculation obtained by the software Flac, whose failure has covered a significant part of the urbanized area (Figure 18, 20 and 21b). In any case, the results of both calculations are consistent with regards to the volume, the thickness, and the nature of the lands set in motion.
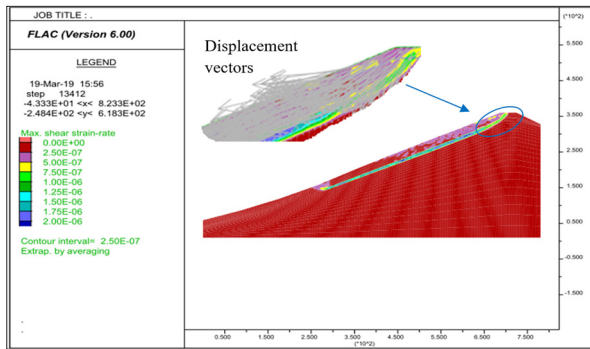
Figure 20. Failure mechanism 3 (Moderate piezometric height).

7.4. Failure Mechanism 4

The sliding spreads over a larger part of the slope which shows a mobilization of a thick slice of the substratum (Figure 22). It appears that the lower is the cohesion of the substratum, and the greater is the depth of failure. It is worth noting that this configuration represents the presence of a thick layer of a crushed schist or the presence of poor mechanical characteristics where discontinuities appear. Current knowledge tends to show that this deformation mode seems to be very unrealistic. It shows, however, that the mode of failure depends explicitly on the current mechanical strength of the rock. Therefore, precise knowledge of the current geological structure of the rock massifs should provide answers to this question regarding the possibility of failure or a very deep potential failure.
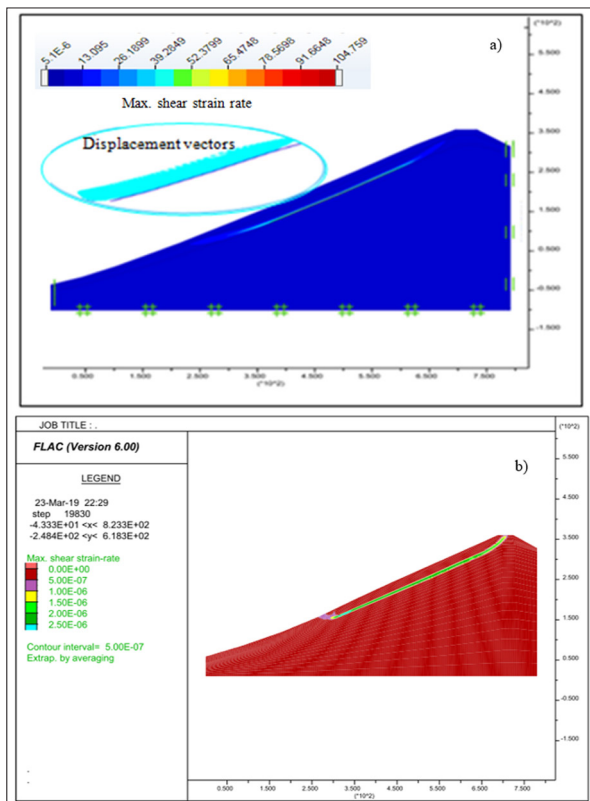
Figure 21. Comparison between the results of the two softwares a) limit analysis. b) finite difference analysis (low piezometric height).
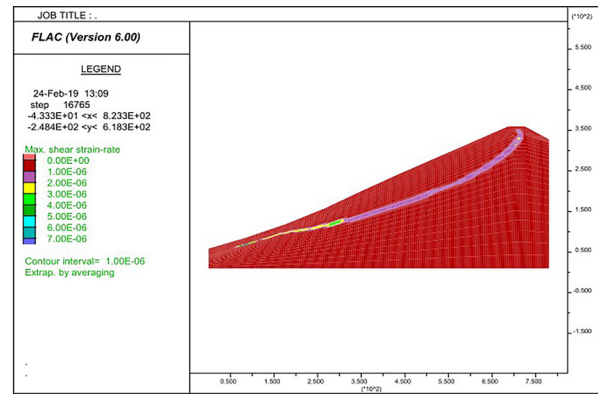
Figure 22. Failure mechanism 4 (Average drainage level and low cohesion)

8. Conclusions

The stability analysis carried out on the slope of Ain El Hammam shows that the failure occurred in the layer of the altered schist. This was confirmed by the in-situ observations and also by the analysis of the surveys carried out on site. Several conclusions, remarks, and parameters are issued from this study, the most important of which include:

- The main motor generating this movement is water. High interstitial pressures at the sliding surface combined with high inclination and an overload upon the slope caused movements of the slope. The critical phases are closely related to the increase in hydraulic potentials within the slope.
- The evolution of the displacements obtained by the simulations with hydraulic conditions which reflect "real ones" gives orders of magnitude that are very coherent with the real ones. In addition, the spatial distribution of active areas is very similar to that observed in the site.
- The variation of the angle of friction at the level of the rocky massifs has no influence on the stability of the slope.
- The substantial increment of the cohesion factor C leads to an improvement of stability, but this improvement remains very limited and essentially dependant on the level of the water table.
- The effect of the urbanization load is remarkable not only by the excessive variation of the intensity of the maximum displacement, but also by the modification of the distribution of the isovalue fields of displacements.
- The variation of the four main rupture configurations depends mainly on the drainage conditions and the cohesion allocated for the rock mass.

References

ANTEA-HYDROENVIRONNEMENT-TTI. (2010). Étude du glissement de terrain d'Ain El Hammam – Rapport n°1, Mission A, mars 2010, N° 57665/A.

Bemani Yazdi, P. (2009). Modélisation de la stabilité des massifs rocheux avec prise en compte de l'endommagement des joints et des effets hydromécaniques. Mécanique des matériaux [physics.classph]. Ecole des Ponts ParisTech, 2009. Français. ffNNT : 2009ENPC0921ff. ffpastel-00662311f

Billaux, D., and Dedecker, F. (2018). Modélisation numérique des roches et fracturation : du continu au discontinu, Revue Française de Géotechnique, 155, 2.

Bouaziz, N., and Melbouci, B. (2019). Characterization of Illilten earth flow (Algeria). Bulletin of Engineering Geology and environment, 18(1): 669-689.

CENEAP-MATET. (2010). Étude relative a la délimitation et a la caractérisation des zones de montagne et des massifs montagneux du Djurdjura, phase n°2 : analyse prospective de l'état des lieux du massif, version corrigée n°3.

Chalhoub, M. (2010). Massifs rocheux : Homogénéisation et classification numériques, Mines Paris ParisTech Les presses.

Cubas, N. (2009). Séquences de chevauchement, prédictions mécaniques, validation analogique et application `à la chaîne de l'Agrio, Argentine, Thèse de doctorat Université Paris XI.

Dadouche, F., Belabed, L., Zennir, A. (2008). Analyse probabiliste de la stabilité des talus vis-à-vis du glissement, International Conférence on Computation in Geotechnical Engineering NUCGE'08, pp. 130-135.

Dapples, F. (2002). Instabilités de terrain dans les Préalpes fribourgeoises (Suisse) au cours du Tardiglaciaire et de l'Holocène: influence des changements climatiques, des fluctuations de la végétation et de l'activité humaine, Thèse de doctorat, Université de Fribourg (Suisse).

Djerbal, L., and Melbouci, B. (2013). Contribution to the mapping of the landslide of Ain El Hammam (Algérie), Advanced Materials Research, 601: 332-336.

Djerbal, L., and Melbouci, B. (2012). Le glissement de terrain d'Ain El Hammam (Algérie) : causes et évolution, Bulletin of Engineering Geology and the Environment, 71: 587-597.

Durand-Delga, M. (1969). Mise au point sur la structure du nord est de la Berbérie, Publ. Serv. Geol. Algérie n° 3, pp. 89-131.

Faure, R.M. (2000). L'évolution des méthodes de calcul en stabilité des pentes, Partie I : Méthodes à la rupture, Revue française de géotechnique N° 92 3ème trimestre, pp. 3-6.

Fleurisson, A. (2001). Structures géologiques et stabilité des pentes dans les massifs rocheux: description, analyse et modélisation, Revue française de géotechnique N° 95/96 2ème et 3ème trimestre 2001, pp. 103-116.

GEOMICA. (2006). Rapport Interne- Étude géotechnique de la zone de glissement et de tassement d'Ain El Hammam, Travaux de la phase I.

GEOMICA. (2009). Rapport Interne -Étude géotechnique de la zone de glissement et de tassement d'Ain El Hammam, Travaux de la phase II.

Gravanis, E., Pantelidis, L. Griffiths, D.V. (2014). An analytical solution in probabilistic rock slope stability assessment based on random fields, Int. J. Rock Mech. Min. Sci., 71: 19-24.

Guirous, L., Dubois, L., Melbouci, B. (2014). Contribution à l'étude du mouvement de terrain de la ville de Tigzirt (Algérie), Bulletin of Engineering Geology and environment, 73(4): 971-986.

Ietto, F., Perri, F., Cella, F. (2018). Weathering characterization for landslides modeling in granitoid rock masses of the capo Vaticano promontory (Calabria, Italy), Landslides, 15: 43-62.

Ismail, E.H., Rogers, J.D., Ahmed, M.F., Usery, E.L., Abdelsalam, M.G. (2017). Landslide susceptibility mapping of Blue Nile and Tekeze River Basins using oblique rainfall-aspect rasters. Bull. Eng. Geol. Environ. 2017, 1–19.

Kechidi, Z. (2010). Application des études minéralogiques et géotechniques du schiste au glissement de terrain d'Ain El Hammam, Mémoire Master, université de Tizi-Ouzou (Algérie).

Li, D.Q, Zheng, D., Cao, Z.J., Tang, X.S., Phoon, K.K. (2016). Response surface methods for slope reliability analysis: review and comparison, Eng. Geol., 203: 3-14.

LNTPB. (1973). Rapport Interne -Marché de Ain El Hammam, étude géologique et géotechnique du glissement.

Michalowski, R.L. (1995). Slope stability analysis: a kinematical approach. Geotechnique, 45(2): 283-293.

Pisani, G., Castelli M., Scavia C. (2010) Hydrogeological model and hydraulic behavior of a large landslide in the Italian Western Alps. Nat Hazards Earth Syst Sci 10:2391–2406

Tullen, P. (2002). Méthodes d'analyse du fonctionnement hydrogéologique des versants instables, Thèse de doctorat, École Polytechnique Fédérale de Lausanne.

Wu, L.Z., Liu, G.G., Wang, L.C., Zhang, L.Min., Li, B.E., Li, B. (2016). Numerical analysis of 1D coupled infiltration and deformation in layered unsaturated porous medium, Environ Earth Sci., 75 (9).

Wu, Q., Tang, H., Ma, X., Wu, Y., Hu, X., Wang, L., Criss, R., Yuan, Y., Xu Y. (2019). Identification of movement characteristics and causal factors of the Shuping landslide based on monitored displacements. Bulletin of Engineering Geology and the Environment, 78: 2093-2106.